Particle Filter ROV Navigation using Hydroacoustic Position and Speed Log Measurements

Bo Zhao, Mogens Blanke, and Roger Skjetne

***Abstract*— An integrated navigation system design is presented for an underwater remotely operated vehicle (ROV). The available navigation information is an acoustic position measurement and a Doppler log speed measurement. Both measurements are studied in detail and modeled statistically. A kinematic model is assigned to the ROV with its driving noise from a Gaussian mixture, and a particle filter is suggested to estimate ROV position and velocity.**

The advantages of using a particle filter in this ROV navigation scheme are: 1) to make full use of all available information to improve the estimation performance, such as the speed measurement that is a nonlinear function of the states; 2) the particle filter makes good use of a Gaussian mixture as the driving noise, which makes the ROV kinematic model more realistic in both high and low frequency ranges; 3) a good estimate of the ROV velocity vector is achieved. The algorithm of the particle filter is presented and verified through a simulation based on real data. This shows that the estimation performance of the particle filter is clearly better than that of a Kalman filter.

I. Introduction

In the past decades, more and more remotely operated underwater vehicles (ROVs) have emerged in marine operations, such as offshore hydrocarbon production and ocean scientific exploration. An ROV is a tethered underwater vehicle, connected with a support surface vessel with power supply and signal transmission cables through an umbilical. Typically, the support vessel is equipped with a dynamic positioning (DP) system, which controls the vessel to maintain a desired position. The ROV is controlled from a command center installed onboard the support vessel. Since the ROV is controlled relatively to the support vessel, the relative position and velocity states of the ROV must be obtained as accurately as possible through an ROV navigation system involving appropriate measurements and navigation filters.

There are several sensors for measuring the kinematic variables of an ROV; see for instance the review in [1] where different sensors are classified by their usage and discussed according to measuring principles and levels of accuracy. In [2], the pros and cons regarding the acoustic measurement and Doppler log measurement for ROV navigation is discussed. Kalman filters or complementary filters are good estimators if the position, orientation, and possibly velocity measurements are available. When no speed measurements are available, model-based estimators are generally used.

The particle filter (PF) has drawn great attention since it was proposed in [3], due to its ability to solve optimal estimation problems in nonlinear non-Gaussian scenarios. After being introduced by [3], the PF solutions have been enriched by [4], [5], and others. Later, a constructive tutorial for PF designs was presented by [6], and more recently a PF review was provided in [7]. As of today, the PF has been successfully applied in applications including target tracking, computer vision, digital communications, speech recognition, machine learning, and other areas as reported in [8].

The contribution of this paper is an ROV navigation scheme based on a particle filter that can be summarized as follows:

- A particle filter is designed and applied as a navigation filter instead of a Kalman filter to take advantage of all measurements, including the Doppler speed log being a nonlinear function of the linear velocities, in order to improve the estimation performance and robustness.
- Detailed statistical models for the position and speed sensors are derived, based on real data, and applied in the design. This ensures effective attenuation of position and speed measurements noise without having a kinetic model of the ROV available.
- As the solution is based only on a hydroacoustic position measurement and a Doppler speed log, the proposed design can be applied as a redundant ROV state estimator in addition to other state-of-the-art methods.

II. Navigation Objective

A. System Description

The navigation problem considered here was motivated by full-scale ROV experiments conducted at the Applied Underwater Robotics Laboratory (AUR-Lab) at NTNU. The AUR-Lab has access to NTNU's research vessel R/V Gunnerus and the ROV Minerva, for which the aim is to develop new technology for marine monitoring and ocean observation. A short term goal for the AUR-Lab is to develop an ROV control system with user interface, having 3D dynamic positioning (DP) and tracking capabilities for use in ROV research missions. Essential to this development is to design a robust and high-performing ROV navigation system based on a minimum number of sensors operating in a real environment.

Bo Zhao is Ph.D. candidate at the Centre for Ships and Ocean Structures (CeSOS), Norwegian University of Science and Technolog (NTNU), 7491 Trondheim, Norway bo.zhao@ntnu.no

Mogens Blanke is Professor at the Technical University of Denmark, 2800 Kgs Lyngby, Denmark and Adjunct Professor at Norwegian University of Science and Technology, 7491 Trondheim, Norway mb@elektro.dtu.dk

Roger Skjetne is Professor at the Department of Marine Technology, Norwegian University of Science and Technolog (NTNU), 7491 Trondheim, Norway roger.skjetne@ntnu.no

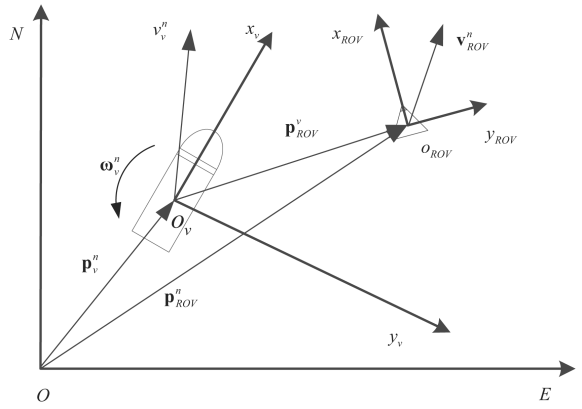

Fig. 1. The configuration of the ROV-vessel system.

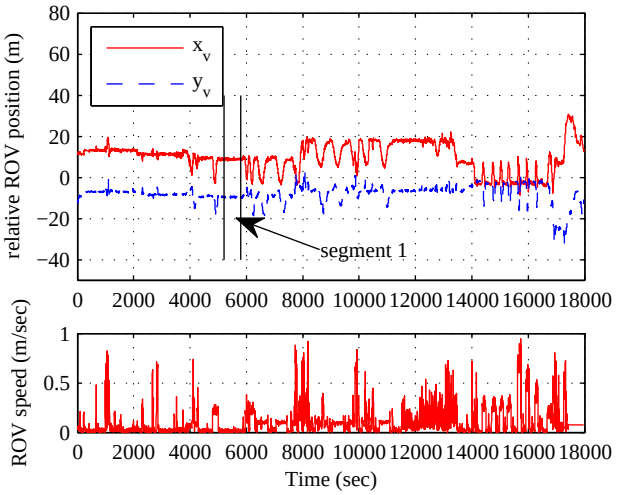

Fig. 2. Time history of SSBL acoustic positioning system and the Doppler speed log measurement.

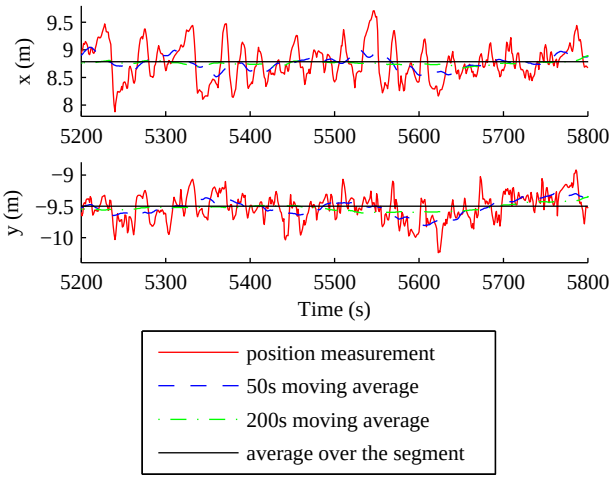

Fig. 3. Position measurements from the stationary segment between 5200 s and 5800 s. The position measurements, moving averages with window sizes of 50 s and 200 s, and the mean values over the whole period.

The operational setup is to use the R/V Gunnerus as a support vessel, performing stationkeeping or low-speed tracking, while the ROV Minerva is controlled from an onboard command station. Several navigation sensors are installed on the ROV Minerva, such as a depth sensor, a fluxgate compass, a Super-Short Base Line (SSBL) hydroacoustic positioning system, and a Doppler speed log. Only the horizontal motions of the vessels are of interest, and Figure 1 shows the relevant reference frames and corresponding position and velocity vectors. The position of the support vessel is represented in the earth-fixed North-East (NE) frame, and the corresponding vectors are indicated with a superscript 'n'. A vessel-fixed frame (V) for the support vessel is indicated by a superscript 'v' and defined with origin at a given fixed center point O_v in the vessel (typically midships and waterline), the x_v-axis in the longitudinal direction, and the y_v-axis in the transversal direction. The position and linear velocity of the ROV in the NE-frame are given by $\mathbf{p}_{ROV}^n$ and $\mathbf{v}_{ROV}^n$, respectively, while $\mathbf{p}_{ROV}^v$ and $\mathbf{v}_{ROV}^v$ are the corresponding vectors in the (V)-frame. Since only the position and linear velocities of the ROV are of interest in this navigation design, the orientation and angular velocity are not considered.

The ROV control system has been tested in several missions and different test scenarios. The data set considered in this paper, named "110228G002", is an approximate 5 hour long mission record. During that period, the R/V Gunnerus was in stationkeeping mode and the maneuvering control system for the ROV Minerva was tested. The DP system for the support vessel provides accurate and reliable estimates of the vessel's position $\mathbf{p}_v^n$, orientation, and corresponding velocities [9].

B. Problem Statement

The problem considered in this paper is to robustly and accurately estimate the relative position $\mathbf{p}_{ROV}^v$ and linear velocity $\mathbf{v}_{ROV}^v$ of the ROV based on only a relative SSBL hydroacoustic position measurement and a Doppler speed log measurement. The ROV heading is not available. As can be seen from Figure 2, these measurements contain significant levels of noise and disturbances that the design must account for.

III. Statistical Modeling of Measurements

A. SSBL Hydroacoustic Position Reference

The position of the ROV is measured by an SSBL acoustic system, with an example of the measurements shown in Figure 2. The motion of the ROV in this data set is a composition of stationary and maneuvering segments. If the position of the ROV has no significant changes during a period, this segment is termed *stationary*. In order to analyze the statistical characteristics of the measurement noise, a time-window with stationary behavior is selected and plotted in Figure 3.

Figure 3 also shows different moving average curves, and the means of the position measurements during the segment. The PSD clearly has a lowpass character with a bandwidth of 0.2 rad/s. The error ellipse in position error has axes $(0.33\,m)^2$ and $(0.22\,m)^2$. This is close the to theoretical

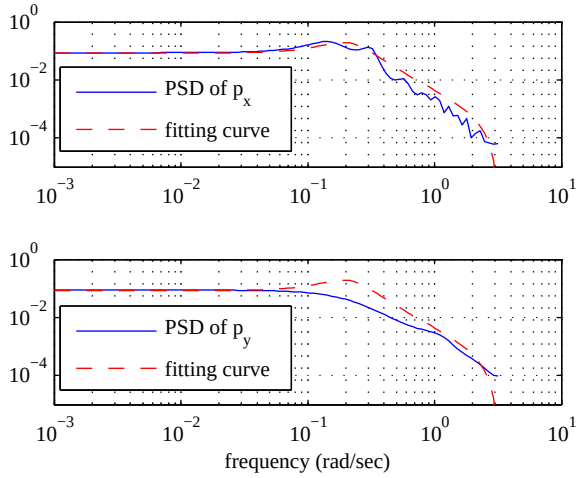

Fig. 4. The power spectrum density (PSD) analysis of the position measurement signal in x and y direction, respectively.

values of the SSBL measurement itself, and it can be concluded that the ROV position is stationary during the segment, implying that the variation is due to measurement noise and system noise. This conclusion is also reached by analyzing the power spectrum density (PSD) of position measurements, as shown in Figure 4. Since the magnitudes of the PSD curves at low frequency are below $10^{-0.8} dB$, it is concluded that the ROV has no significant low frequency motion and is therefore stationary in this segment.

The PSD in Figure 4 shows that the measurement signal is a colored lowpass filtered noise. In addition, the shapes of the power spectrum density curves are not the same, such that the auto-correlation functions of the measurement noise in the x_v and y_v directions are different in at least this segment. However, considering the measuring principle of SSBL, the measurement noise is supposed to be isotropic. So, for simplicity of design, only a single fitting curve is used to approximate these two PSD curves:

$$G_{\text{fitting}}(z) = \frac{0.001203\,(z+1)^2\,(z-0.8182)^2}{(z^2-1.761z+0.8039)^2}. \qquad (1)$$

The sampling frequency is $1Hz$, which is the update frequency of the acoustic measurement.

A stochastic process that generates this PSD is obtained as $H(z)$ where $H(z)H^*(z) = G_{\text{fitting}}(z)$,

$$H(z) = \frac{0.0343\,(z+1)\,(z-0.8182)}{z^2-1.761z+0.8039}, \qquad (2)$$

This transfer function is realized in state-space form as

$$\xi_{k+1} = \mathbf{A}_\zeta \xi_k + \mathbf{B}_\zeta w_k \qquad (3)$$

$$\zeta_k = \mathbf{C}_\zeta \xi_k + \mathbf{D}_\zeta w_k, \qquad (4)$$

where ξ the intermediate states; w_k is a white noise sequence of unit variance; and ζ is the colored noise output sequence. Moreover, $\mathbf{A}_\zeta = \begin{bmatrix} 1.7608 & -0.8039 \\ 1 & 0 \end{bmatrix}$, $\mathbf{B}_\zeta = \begin{bmatrix} 1 \\ 0 \end{bmatrix}$, $\mathbf{C}_\zeta = \begin{bmatrix} 0.0667 & -0.0557 \end{bmatrix}$, and $\mathbf{D}_\zeta = 0.0343$.

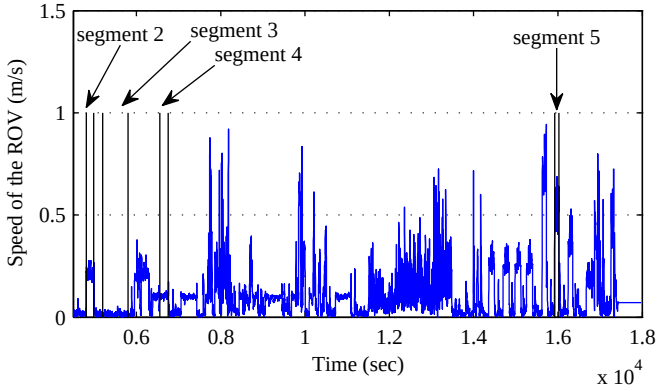

Fig. 5. Four segments are picked from the test data set, assuming the speed of the ROV is constant in each of these segments. The time intervals of the segments are listed in Table I.

B. Doppler Speed Log Measurement

In the NE frame, the ROV velocity is denoted as

$$\mathbf{v}^n_{ROV} = \begin{bmatrix} v^n_{ROV,N} \\ v^n_{ROV,E} \end{bmatrix}, \qquad (5)$$

where $v^n_{ROV,N}$ and $v^n_{ROV,E}$ are the velocity of the ROV in the north and east directions, respectively, and $s_D = \left\|\mathbf{v}^n_{ROV}\right\|_2$ is the corresponding speed. For the speed measurement two assumptions have to be made: 1) there is no correlation between the measurement noise in the different directions, and 2) the variances of the measurement noises in the different directions are equal. Then the speed measurement can be seen as a normal random vector with expectation $\mathbf{v}^n_{ROV}$ and covariance matrix Σ, that is

$$\mathbf{v}_D \sim \mathbf{N}(\mathbf{v}^n_{ROV}, \Sigma), \qquad (6)$$

where Σ is diagonal with identical diagonal entries. For a Doppler log, the noise in the measurement increases with the speed [10]. Therefore,

$$\Sigma(\|\mathbf{v}^n_{ROV}\|_2) = \begin{bmatrix} \sigma^2_D\left(\left\|\mathbf{v}^n_{ROV}\right\|_2\right) & 0 \\ 0 & \sigma^2_D\left(\left\|\mathbf{v}^n_{ROV}\right\|_2\right) \end{bmatrix}, \qquad (7)$$

where σ^2_D is the variance of the Doppler speed log measurement in one direction.

As mentioned, this experiment suffers from the lack of a heading measurement. Therefore, the only helpful information to this navigation problem from the Doppler log is the nonlinear speed measurement $s_D = \|\mathbf{v}_D\|_2$. It is deduced from the normality distribution assumption of the velocity measurement that the speed measurement is a Rice distributed random variable, that is $s_D \sim \text{Rice}\left(\left\|\mathbf{v}^n_{ROV}\right\|_2, \sigma_{v,D}\left(\left\|\mathbf{v}^n_{ROV}\right\|_2\right)\right)$.

To model the distribution of the speed measurement, the main task is to formulate the function $\sigma_{v,D}\left(\left\|\mathbf{v}^n_{ROV}\right\|_2\right)$. Here we also pick up some segments from the whole measurement as shown in Figure 5. The means and variances of the speed measurements in these segments are listed in Table I.

A Rice distributed variable $x \sim \text{Rice}(\delta, \sigma)$, has δ as the *distance parameter* and σ as the *scale parameter*. The Rice

TABLE I

STATISTICAL PROPERTIES OF DIFFERENT SPEED MEASUREMENT SEGMENTS

Segment	Time interval	Mean	Variance	δ	σ
2	[4810, 4980]	0.217	0.024^2	0.22	0.024
3	[5200, 5800]	0.014	0.0079^2	≈ 0	0.012
4	[6550, 6750]	0.103	0.0085^2	0.10	0.009
5	[15925, 16020]	0.545	0.066^2	0.54	0.066

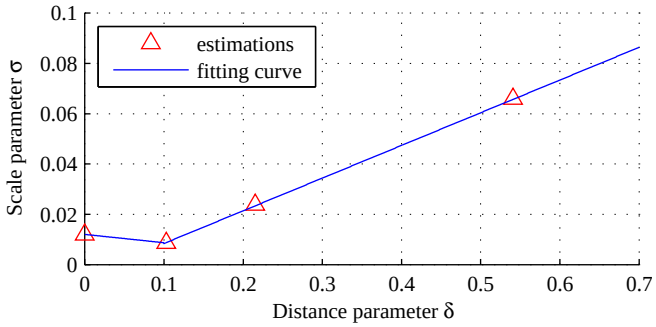

Fig. 6. The estimated (δ, σ) pair in four segments, and straight line fitting.

PDF is

$$f(x|\delta,\sigma) = \frac{x}{\sigma^2}\exp\left(-\frac{(x^2+\delta^2)}{2\sigma^2}\right) I_0\left(\frac{x\delta}{\sigma^2}\right), \qquad (8)$$

where $I_k(z)$ is the modified Bessel function of the first kind of k'th order.

A method to estimate the Rice parameters recursively was shown in [11]. Following this method, the estimations of the parameters of each segment are obtained and shown in Table I. To obtain the whole expression of $\sigma_D\left(\left\|\mathbf{v}^n_{ROV}\right\|_2\right)$, we use two linear segments to fit the four estimated (δ, σ) pairs, as shown in Figure 6. The feature that the Doppler log measurement noise increases with the speed coincides with the technical specification in [12]. The analytical expression of $\sigma_{v,D}\left(\left\|\mathbf{v}^n_{ROV}\right\|_2\right)$ is

$$\sigma_{v,D}(\|\mathbf{v}\|_2) = \begin{cases} 0.012 - 0.0331\|\mathbf{v}\|_2 & , \ 0 \le \|\mathbf{v}\|_2 < 0.1 \\ -0.0046 + 0.130\|\mathbf{v}\|_2 & , \ 0.1 \le \|\mathbf{v}\|_2 \end{cases}. \qquad (9)$$

IV. ROV MODEL AND NAVIGATION SYSTEM DESIGN

A. ROV Kinematic Model

Since the thrust of the ROV is not measured in the experiment, only a noise driving kinematic model is available. Taking the ROV position $\mathbf{p}^v_{ROV}$, velocity $\mathbf{v}^v_{ROV}$, and acceleration $\mathbf{a}^v_{ROV}$ into consideration, a discrete ROV kinematic model is

$$\begin{bmatrix} \mathbf{p}^v_{ROV,k+1} \\ \mathbf{v}^v_{ROV,k+1} \\ \mathbf{a}^v_{ROV,k+1} \end{bmatrix} = \begin{bmatrix} \mathbf{I} & \mathbf{I} & \frac{1}{2}\mathbf{I} \\ \mathbf{0} & \mathbf{I} & \mathbf{I} \\ \mathbf{0} & \mathbf{0} & \mathbf{I} \end{bmatrix} \begin{bmatrix} \mathbf{p}^v_{ROV,k} \\ \mathbf{v}^v_{ROV,k} \\ \mathbf{a}^v_{ROV,k} \end{bmatrix} + \begin{bmatrix} \frac{1}{6}\mathbf{I} \\ \frac{1}{2}\mathbf{I} \\ \mathbf{I} \end{bmatrix} \mathbf{w}_{a,k}. \qquad (10)$$

with sampling frequency $1\,Hz$ as the update frequencies of the measurements, and $\mathbf{w}_{a,k}$ is a white driving noise. This model assumes that the support vessel is stationary and thereby constitutes an inertial frame, which is an acceptable assumption because the support vessel is in station keeping mode during the experiment. The ROV kinematic model is written compactly as

$$\eta^v_{k+1} = \mathbf{A}_\eta \eta^v_k + \mathbf{B}_\eta \mathbf{w}_{a,k}, \qquad (11)$$

where $\eta^v_k = \begin{bmatrix} \mathbf{p}^v_{ROV,k} & \mathbf{v}^v_{ROV,k} & \mathbf{a}^v_{ROV,k} \end{bmatrix}^\top$ is the general kinematic state vector of the ROV, and $\mathbf{A}_\eta$ and $\mathbf{B}_\eta$ follow from Equation (10).

As shown in Figure 2, the ROV motion is a combination of stationary and maneuvering sections. In order to enhance the tracking performance, it is necessary to assign a flexible distribution to the driving noise $\mathbf{w}_a$, making the model dynamics more realistic. By differencing the position measurement twice, an estimation of the ROV acceleration is obtained and shown in Figure 7, including a corresponding Gaussian mixture fitting curve. The Gaussian mixture is formulated as

$$\mathbf{w}_{a,k} \sim mix\begin{bmatrix} 0.7826 \cdot N\left([0,0]^\top, 6.89\times10^{-5}\mathbf{I}\right) \\ 0.2174 \cdot N\left([0,0]^\top, 0.049\mathbf{I}\right) \end{bmatrix}. \qquad (12)$$

The operator $mix[\cdot]$ is a mixing operator defined as of probability density functions. For a vector of weighted probability density functions $\mathbf{f} = \begin{bmatrix} w_1 f_1(x) & w_2 f_2(x) & \cdots & w_n f_n(x) \end{bmatrix}^\top$, where w_i $(i = 1, \cdots, n)$ are the weights satisfying $\sum_i w_i = 1$, and $f_i(x)$ are the probability density functions on the same support set. The mixing operator gives a probability density function $mix[\mathbf{f}] = \sum_i w_i f_i(x)$.

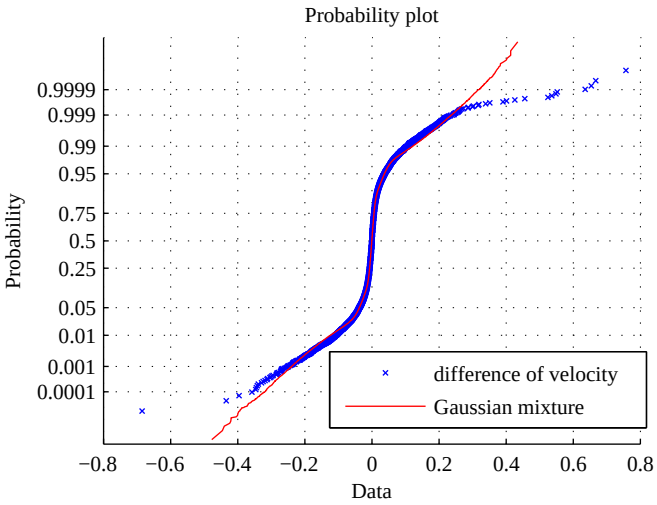

Fig. 7. Probability plot of data and a Gaussian mixture fitting. The Gaussian mixture distribution fits data very well in the probability range 0.001 to 0.999. Tails are wider than Gaussian but this not essential for this application.

B. Modeling of the measurement

1) SSBL Acoustic Measurement: Following the equations (3) and (4), the SSBL acoustic measurement is modeled as

$$\xi^+_{k+1} = \mathbf{A}^+_\zeta \xi^+_k + \mathbf{B}^+_\zeta \mathbf{w}_{\zeta,k} \qquad (13)$$

$$\zeta^+_k = \mathbf{C}'^+_\zeta \xi^+_k + \mathbf{D}^+_\zeta \mathbf{w}_{\zeta,k} \qquad (14)$$

$$\mathbf{p}^v_{A,ROV,k} = \mathbf{p}^v_{ROV,k} + \zeta^+_k, \qquad (15)$$

where $\mathbf{p}^v_{A,ROV,k}$ is the acoustically measured position at time instance k. ξ^+_k, ξ^+_{k+1}, and ζ^+_k are the vertically tile expansion of ξ_k, ξ_{k+1}, and ζ_k. $\mathbf{A}^+_\zeta$, $\mathbf{B}^+_\zeta$, $\mathbf{C}'^+_\zeta$, and $\mathbf{D}^+_\zeta$ are 2-by-2 block diagonal matrixes of $\mathbf{A}_\zeta$, $\mathbf{B}_\zeta$, $\mathbf{C}_\zeta$, and $\mathbf{D}_\zeta$, respectively. $\mathbf{w}_{\zeta,k}$ is a two dimensional white noise vector with independent components and unit variance for each.

2) Doppler Log Measurement: The speed measurement from the Doppler log is modeled as a Rice distributed random variable, such that $s_D \sim \text{Rice}\left(\left\|\mathbf{v}^n_{ROV}\right\|_2, \sigma_{v,D}\left(\left\|\mathbf{v}^n_{ROV}\right\|_2\right)\right)$, where $\sigma_{v,D}\left(\left\|\mathbf{v}^n_{ROV}\right\|_2\right)$ is formulated in (9). It follows that the speed measurement from the Doppler log can be expressed as

$$s_k = s_{D,k}. \tag{16}$$

C. Particle filter design

Combining the system model and the measurement model yields the following model of the ROV

$$\begin{aligned}\begin{bmatrix}\xi^+_{k+1}\\ \eta^v_{k+1}\end{bmatrix} &= \begin{bmatrix}\mathbf{A}^+_\zeta & \mathbf{0}\\ \mathbf{0} & \mathbf{A}_\eta\end{bmatrix}\begin{bmatrix}\xi^+_k\\ \eta^v_k\end{bmatrix}\\ &\quad + \begin{bmatrix}\mathbf{B}^+_\zeta & \mathbf{0}\\ \mathbf{0} & \mathbf{B}_\eta\end{bmatrix}\begin{bmatrix}\mathbf{w}_{\zeta,k}\\ \mathbf{w}_{a,k}\end{bmatrix} \qquad (17)\\ \begin{bmatrix}\mathbf{p}^v_{A,ROV,k}\\ s_k\end{bmatrix} &= \begin{bmatrix}\mathbf{C}'^+_\zeta & \mathbf{C}_\eta\\ \mathbf{0} & \mathbf{0}\end{bmatrix}\begin{bmatrix}\xi^+_k\\ \eta^v_k\end{bmatrix}\\ &\quad + \begin{bmatrix}\mathbf{D}^+_\zeta & \mathbf{0}\\ \mathbf{0} & \mathbf{0}\end{bmatrix}\begin{bmatrix}\mathbf{w}_{\zeta,k}\\ \mathbf{w}_{a,k}\end{bmatrix} + \begin{bmatrix}0\\ 1\end{bmatrix} s_{D,k}, \qquad (18)\end{aligned}$$

where $\mathbf{C}_\eta = \begin{bmatrix}\mathbf{I} & \mathbf{0} & \mathbf{0}\end{bmatrix}^\top$ and $s_{D,k} \sim \text{Rice}\left(\left\|\mathbf{v}^v_{ROV,k}\right\|_2, \sigma_{v,D}\left(\left\|\mathbf{v}^v_{ROV,k}\right\|_2\right)\right)$. For compactness, the system model in (17) and (18) is given by

$$\begin{aligned}\mathbf{x}_{k+1} &= \mathbf{A}\mathbf{x}_k + \mathbf{B}\mathbf{w}_k \qquad (19)\\ \mathbf{y}_k &= \mathbf{C}\mathbf{x}_k + \mathbf{D}\mathbf{w}_k + \mathbf{F}s_{D,k}. \qquad (20)\end{aligned}$$

Because some of the noise terms are non-Gaussian and one measurement is nonlinear, which violates the assumptions of a Kalman filter, a particle filter is proposed to solve the problem. The PF algorithm partially follows the sampling importance resample particle filter in [6], and is given by

Algorithm Particle filter for ROV navigation

1) **Initializing:** At time l, initialize the particles deterministically, such as $\mathbf{x}^i_{l-1} = \left[\mathbf{0}_{4\times1}\ \left(\mathbf{p}^n_{A,ROV,l-1}\right)^\top\ \mathbf{0}_{4\times1}\right]^\top$ $(i = 1,\cdots N_s)$, where N_s is the number of particles in the filter. And the weights of the these particles are initialized as $w^i_{l-1} = \frac{1}{N_s}$.
2) **System time update:** At this step, the objective is to draw new particles $\mathbf{x}_{k|k-1}$ with the posterior $\mathbf{p}\left(\mathbf{x}_{k-1}|\mathbf{y}_{1:k-1}\right)$ from last cycle. Introducing the importance density $\mathbf{q}\left(\mathbf{x}_k|\mathbf{x}^i_{k-1},\mathbf{y}_k\right) = \mathbf{p}\left(\mathbf{x}_k|\mathbf{x}^i_{k-1}\right)$, we draw new particles from the importance density $\mathbf{p}\left(\mathbf{x}_k|\mathbf{x}^i_{k-1}\right)$. That is, for $\mathbf{x}^i_{k|k-1} = \left[\xi^+_{k|k-1}\ \eta^v_{k|k-1}\right]^\top$, $\xi^+_{k|k-1}$ is drawn from $\mathbf{N}\left(\mathbf{A}_\zeta\xi^+_k, \mathbf{B}_\zeta\mathbf{B}^\top_\zeta\right)$, and $\eta^v_{k|k-1}$ is drawn from (11). Note that the noise terms are randomly generated according to their PDFs.
3) **Measurement update:** At this step, the measurement is used to update the weights of the particles. Since the importance density has been chosen as $\mathbf{q}\left(\mathbf{x}_k|\mathbf{x}^i_{k-1},\mathbf{z}_k\right) = \mathbf{p}\left(\mathbf{x}_k|\mathbf{x}^i_{k-1}\right)$, the update process of the weights will be $w^i_k \propto w^i_{k-1}\Pr\left(\mathbf{y}_k|\mathbf{x}^i_k\right)$. For the PF in this paper, the $\Pr\left(\mathbf{y}_k|\mathbf{x}^i_k\right)$ is analytically expressed as

$$\begin{aligned}&\Pr\left(\begin{bmatrix}\mathbf{p}^v_{A,ROV,k}\\ s_k\end{bmatrix}\middle|\begin{bmatrix}\xi^+_k\\ \eta^v_k\end{bmatrix}^i\right)\\ &= \frac{1}{2\pi\left|\mathbf{D}_\zeta\right|^{\frac{1}{2}}}\\ &\quad\cdot\exp\left\{-\frac{1}{2}\left\|\mathbf{p}^v_{A,ROV,k} - \begin{bmatrix}\mathbf{C}'_\zeta & \mathbf{C}_\eta\end{bmatrix}\left(\xi^+_k\right)^i\right\|_{\left(\mathbf{D}_\zeta\right)^{-1}}\right\}\\ &\quad\cdot\frac{s_k}{\left(\sigma_D\left(\left\|\mathbf{v}^i\right\|_2\right)\right)^2}\exp\left\{-\frac{\left(\left(s_k\right)^2 + \left\|\mathbf{v}^i\right\|_2^2\right)^2}{2\left(\sigma_D\left(\left\|\mathbf{v}^i\right\|_2\right)\right)^2}\right\}\\ &\quad\cdot I_0\left(\frac{s_k\left\|\mathbf{v}^i\right\|_2}{\left(\sigma_D\left(\left\|\mathbf{v}^i\right\|_2\right)\right)^2}\right), \qquad (21)\end{aligned}$$

where $\mathbf{v}^i$ denotes $\left(\mathbf{v}^n_{ROV,k}\right)^i$, and

$$\begin{aligned}&\left\|\mathbf{p}^v_{A,ROV,k} - \begin{bmatrix}\mathbf{C}'_\zeta & \mathbf{C}_\eta\end{bmatrix}\left(\xi^+_k\right)^i\right\|_{\left(\mathbf{D}_\zeta\right)^{-1}}\\ &= \left(\mathbf{p}^v_{A,ROV,k} - \begin{bmatrix}\mathbf{C}'_\zeta & \mathbf{C}_\eta\end{bmatrix}\left(\xi^+_k\right)^i\right)^\top\left(\mathbf{D}_\zeta\right)^{-1}\\ &\quad\cdot\left(\mathbf{p}^v_{A,ROV,k} - \begin{bmatrix}\mathbf{C}'_\zeta & \mathbf{C}_\eta\end{bmatrix}\left(\xi^+_k\right)^i\right). \qquad (22)\end{aligned}$$

In Equation (21) the second term on the right hand side originates from the analytic expression of the Rice distribution.
4) **Resampling:** The PF in this paper uses the residual resampling method proposed by [5], to prevent the degeneracy problem. The procedure is:
   a) For each $i = 1,\cdots,N_s$, return $n_i = \lfloor N_s w^i_k \rfloor$ copies of particle $\mathbf{x}^i_k$.
   b) Let $N_r = N_s - n_1 - \cdots - n_{N_s}$ and get N_r identically and independently distributed draws from $\left\{\mathbf{x}^i_k\right\}$ $(i = 1,\cdots,N_s)$ with probabilities proportional to $N_s w^i_k - k_i$ $(i = 1,\cdots,N_s)$.
   c) Normalize the weights $w^i_k = 1/N_s$.

   As a consequence of the residual resampling method, all the weights of particles are identical to $1/N_s$ at the end of the step.
5) **Go to step 2 and start the next cycle.**

V. Simulation on Experimental Data

The proposed PF based navigation system is verified with the following simulation with experimental data. The estimated ROV position of the PF is compared with the estimations of two different KF based navigation, which is based on the same ROV kinematic model.

The first KF based navigation uses only the SSBL acoustic position measurement. Considering the colored noise, the system equation is also augmented as (13) and (14). This navigation system is referred to as KF#1.

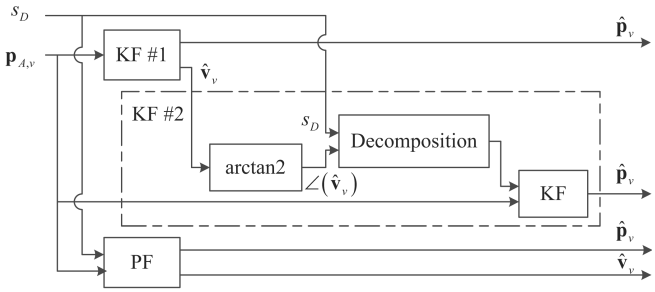

Fig. 8. The structures of the KF#1, the KF#2, and the PF based navigation systems.

A second KF navigation utilizes the KF#1 supplemented with an estimation of direction of the velocity. This is further used to decompose the speed measurement from the Doppler log. Finally, another Kalman filter is used to merge the position measurement and the estimated velocity. This scheme is named KF#2 in the following. The structures of KF#1 and KF#2 are shown in Figure 8.

The simulation uses the entire test data set as input, but only sections of the result are shown in the Figures 9 and 10.

Figure 9 shows the tracking performance of Segment 1, when the ROV was stationary. The PF based navigation has better performance since its estimation oscillates less than KF#1 and KF#2, which means the colored noise in the position measurement is well attenuated. There is bias between the speed measurement and the estimated speed, because when the magnitude of the ROV velocity is small, the effect of the measurement noise dominates the measurement of the Doppler log.

Figure 10 left column shows the tracking performance of the time range $[4000\,\text{sec}, 5000\,\text{sec}]$. During this period, the ROV changed its velocity direction several times. At these points the position estimation of the PF has less overshoot and delay than KFs.

The right column of Figure 10 shows the tracking performance of time range $[15000\,\text{sec}, 16000\,\text{sec}]$, when the ROV switches between stationary and maneuvering. The PF based navigation system responds to the ROV kinematic variation faster than the KFs, and it can still handle well the colored position measurement noise in the stationary sections. The PF based navigation system seem to have better performance than the KF systems in both high and low frequency ranges

VI. Conclusion

This paper described the navigation system design for an ROV. The available information of the ROV was hydroacoustic position and scalar Doppler log speed measurement. The ROV heading and thrust commands were not available. This configuration was shown to require a particle filter rather than a Kalman filter since the speed measurement is a nonlinear non-injective function of the ROV kinematic states.

Based on the configuration of the ROV experiment measurements were studied in detail and modeled. The hydroacoustic positioning system suffers from a colored Gaussian noise, while the speed measurement is modeled as a random variable from a Rice distribution family with scale parameter being a piecewise linear function of the ROV kinematic states. A kinematic model was assigned to the ROV using driving noise from a Gaussian mixture model.

A particle filter was introduced based on the ROV model and the noise model to estimate the position and velocity of the ROV. The algorithm of the particle filter was given and explained in detail. Simulations based on real data showed the estimation from the particle filter to outperform that of traditional Kalman filter approaches. Handling of transients when the ROV motion went from stationary to maneuvering was also found better with the particle filter.

In conclusion, this particle filter-based navigation scheme was able to accurately reconstruct the velocity of the ROV.

Acknowledgement

The data used in this paper is recorded by NTNU Applied Underwater Robotics Laboratory (AUR-Lab), with NTNU's Research vessel R/V Gunnerus and ROV Minerva. Thanks also to the RCN research project 199567, "Arctic DP", for funding the last author.

References

[1] J. C. Kinsey, R. M. Eustice, and L. L. Whitcomb, "A survey of underwater vehicle navigation: Recent advances and new challenges," in *Proceedings of the 7th Conference on Maneuvering and Control of Marine Craft (MCMC 2006)*, Lisbon: IFAC, 2006.

[2] M. Caccia, "Guidance and control of a reconfigurable unmanned underwater vehicle," *Control Engineering Practice*, vol. 8, no. 1, pp. 21-37, Jan. 2000.

[3] N. J. Gordon, D. J. Salmond, and A. F. M. Smith, "Novel approach to nonlinear/non-Gaussian Bayesian state estimation," , in *Radar and Signal Processing, IEE Proceedings For*, vol. 140, no. 2, IET, 1993, pp. 107-113.

[4] G. Kitagawa, "Monte Carlo Filter and Smoother for Non-Gaussian Nonlinear State Space Models", *Journal of Computational and Graphical Statistics*, vol. 5, no. 1, p. 1, Mar. 1996.

[5] J. S. Liu and R. Chen, "Sequential Monte Carlo methods for dynamic systems," *Journal of the American statistical association*, vol. 93, no. 443, pp. 1032C1044, Sep. 1998.

[6] M. S. Arulampalam, S. Maskell, N. Gordon, and T. Clapp, "A tutorial on particle filters for online nonlinear/non-Gaussian Bayesian tracking," , *IEEE Transactions on Signal Processing*, vol. 50, no. 2, pp. 174-188, 2002.

[7] A. Doucet and A. M. Johansen, "A tutorial on particle filtering and smoothing: Fifteen years later," in *Handbook of Nonlinear Filtering*, D. Crisan and B. Rozovsky, Eds. Cambridge: Cambridge University Press, 2009, no. December, pp. 1C39.

[8] Z. Chen, "Bayesian Filtering : From Kalman Filters to Particle Filters , and Beyond," , *Statistics*, pp. 1-69, 2003.

[9] T. I. Fossen, *Handbook of Marine Craft Hydrodynamics and Motion Control.* Wiley, 2011, p. 596.

[10] B. Jalving, K. Gade, K. Svartveit, A. Willumsen, and R. Srhagen, "DVL Velocity Aiding in the HUGIN 1000 Integrated Inertial Navigation System", *Modeling, Identification and Control*, vol. 25, no. 4, pp. 223-236, 2004.

[11] C. G. Koay and P. J. Basser, "Analytically exact correction scheme for signal extraction from noisy magnitude MR signals." *Journal of magnetic resonance*, vol. 179, no. 2, pp. 317-22, Apr. 2006.

[12] Teledyne RD Instruments, "Workhorse Navigator Doppler Velocity Log (DVL)," 2006. [Online]. Available: http://www.rdinstruments.com/datasheets/workhorse_nav_ds_lr.pdf. [Accessed: 18-Dec-2011].

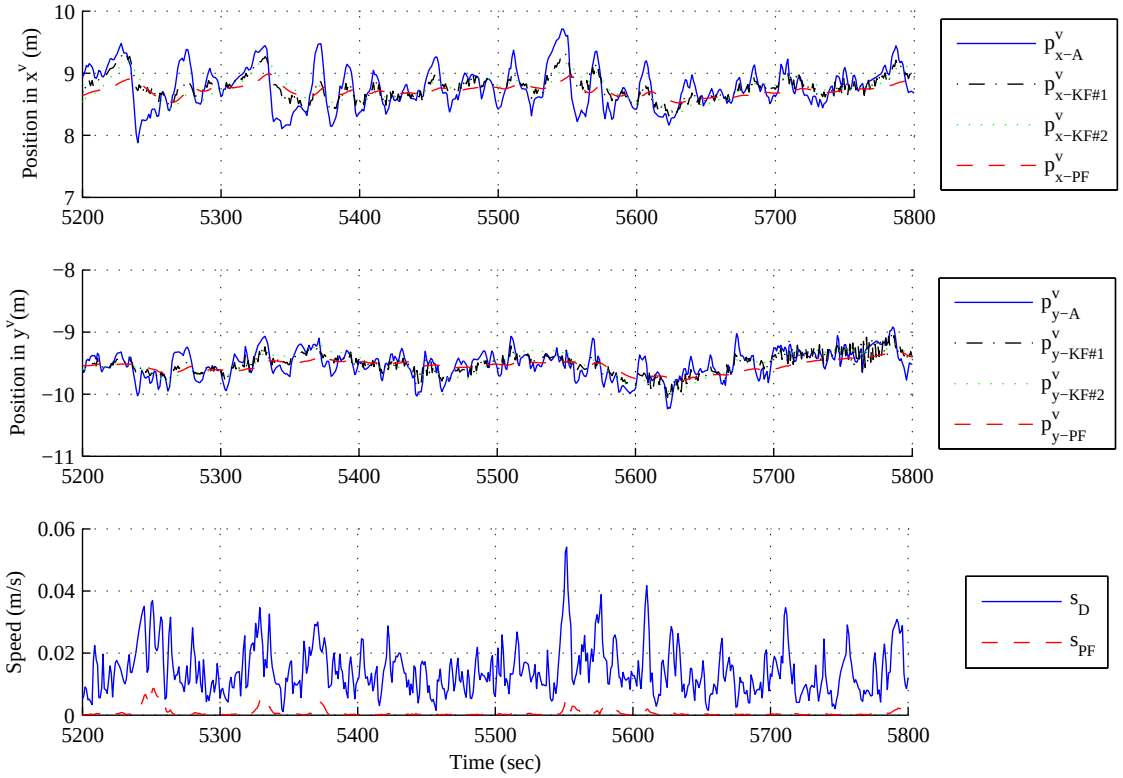

Fig. 9. Tracking performance of time range [5200 sec, 5800 sec].

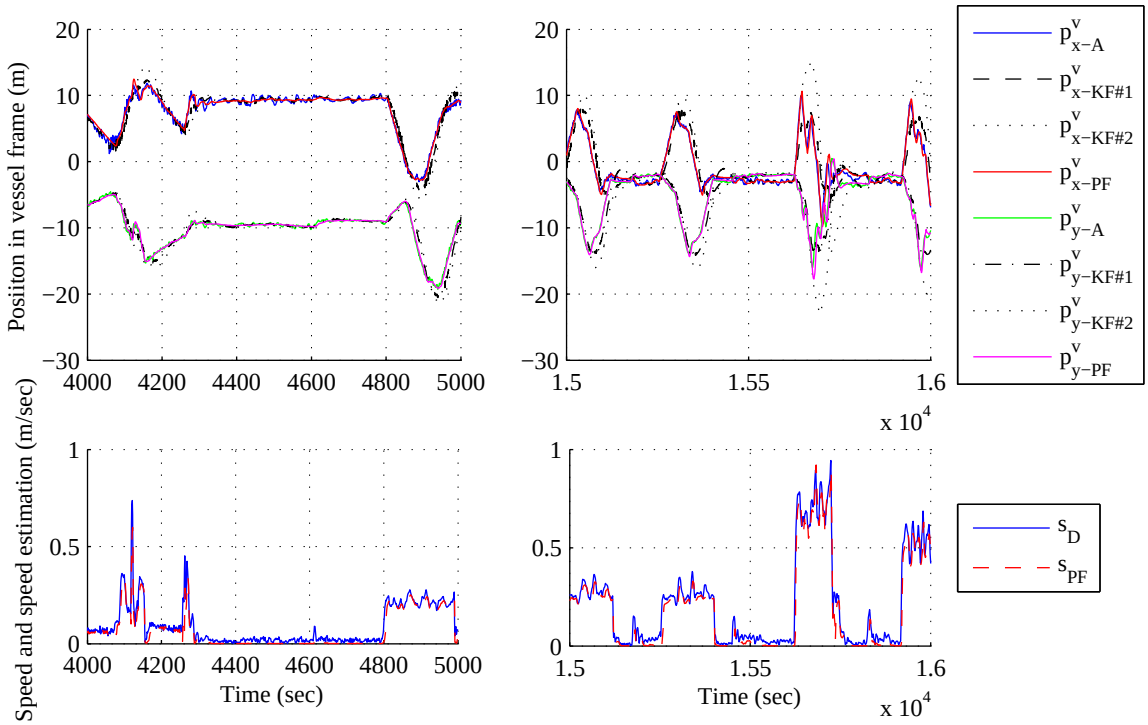

Fig. 10. Tracking performance of time range [4000 sec, 5000 sec], and [15000 sec, 16000 sec].